

# Morphodynamic mechanisms for the formation of asymmetric barchans: improvement of the Bagnold and Tsoar models

Ping Lv<sup>1</sup> · Zhibao Dong<sup>1</sup> · Clement Narteau<sup>2</sup> · Olivier Rozier<sup>2</sup>

Received: 10 March 2015 / Accepted: 3 September 2015  
© Springer-Verlag Berlin Heidelberg 2015

**Abstract** Asymmetric barchan dunes exhibit a marked asymmetry, this morphology develops from the combined effects of two dominant winds, with different directions and relative strengths, and can be described based on Bagnold's and Tsoar's models. In Bagnold's model, the limb nearest to the strongest wind extends and is sustained and enhanced by a gentler wind nearly parallel to the barchan. Tsoar's model expects that the limb farthest from the gentler wind extends in a manner similar to the evolution of seif dunes and that the limb closest to the gentler wind is eroded. To know which model will emerge with variations of the wind, we did some numerical simulations, and found that there exists a critical angle between orientations of the two winds, which decide the formation model of asymmetric barchans. When the angle is greater than this critical value, the effect of the bi-directional winds agrees with Tsoar's model. When the angle is less than the critical value, the evolution of the two horns contradicts Tsoar's model and agrees with Bagnold's model. The critical value for this angle depends on the transport ratio of two winds.

**Keywords** Asymmetric barchans · Strong wind · Gentler wind · Morphodynamic mechanism · ReSCAL model

## Introduction

The development of variation in dune patterns depends strongly on initial conditions that cannot be controlled, such as the wind regime, sand availability, and presence of vegetation, and the asymmetry in these factors reflects that of the dunes (McKee 1979; Lancaster 1995; Kocurek and Ewing 2005; Baas and Nield 2007; Narteau et al. 2009; Bourke 2010; Dong et al. 2010; Lv and Dong 2013, 2014; Lv et al. 2014a, b). For example, barchan dunes form under conditions of limited sand availability and nearly unidirectional or bi-directional winds, usually in areas with low vegetation cover, and because they are so common, they are the most actively studied sand dunes (Finkel 1959; Lancaster 1995; Hesp and Hastings 1998; Hersen 2005; Bourke 2010).

When the wind velocity is greater than a threshold velocity that depends primarily on the characteristics of the surface sediments, sand particles are eroded, transported, and then deposited. Over a short time scale, a pile of sand develops, and the eroded grains from the windward side of the pile are transported to and deposited on the leeward side as a result of separation eddies that form in the recirculation zone downwind of the dune. As this process proceeds, the leeward side becomes steeper until it reaches its angle of repose (about 34°), after which an avalanche occurs; particles fall downhill until the angle of repose is achieved once more. Flow from both sides of the dune carries sand particles to the windward side of the front of the dune, and these particles move faster than the rest of the particles because they are smaller, and this process results in the formation of horns that extend in the wind direction. As a result of these processes, crescentic barchans form, and they move downwind in the direction of the dominant wind through the motion of grains caused by erosion on the windward face and their deposition on the leeward side.

✉ Ping Lv  
lvping@lzb.ac.cn

<sup>1</sup> Key Laboratory of Desert and Desertification, Cold and Arid Regions of Environmental and Engineering Research Institute, Chinese Academy of Sciences, 320 West Donggang Road, Lanzhou 730000, Gansu, China

<sup>2</sup> Laboratoire de Dynamique des Fluides Géologiques, Institut de Physique du Globe de Paris, 4 Place Jussieu, 75252 Paris, Cedex 05, France

Barchans are often asymmetric because the downwind extension of their two limbs differs. Most barchan dunes that form on Earth are asymmetric (Bourke 2010), and similar dunes have been commonly identified on Mars and Titan (Radebaugh et al. 2010). The barchans all have two horns that extend downwind under a specific wind regime, and when the wind regime has two dominant wind directions (i.e., a bi-modal regime), the lengths and widths of the two horns become distinctly different. Asymmetric barchans may subsequently evolve into other dune patterns as their asymmetrical morphodynamic characteristics change; these include linear dunes as well as raked linear dunes (Pye and Tsoar 1990; Dong et al. 2010).

According to Bourke (2010), the limbs that extend downwind can be classified into three groups: linear, beaded, and kinked. The linear horns are generally straight (i.e., they have a single dominant direction), whereas the kinked horns exhibit a distinct angular change in the middle of the horn (the kink); in contrast, the beaded horns resemble a string of beads, with relatively broad, rounded, and high sections that alternate with relatively narrow and low sections.

On Earth, four causes of barchan asymmetry have been identified. The asymmetry may represent a response to bi-directional winds (King 1918; Bagnold 1941; McKee 1966; Tsoar 1984), or the result of collisions between migrating dunes (Hersen 2005), an asymmetrical sediment supply (Rim 1958), or variations in topography (Finkel 1959). During dune collisions, smaller barchans moving downwind collide with one horn of larger barchans that are moving downwind more slowly. In contrast, an asymmetrical sediment supply results in the extension of the horn nearest to the greater sediment supply, and variations in topography block movement of the barchan and produce an asymmetry. However, of these four mechanisms, the responses to a bi-directional wind regime have received the most attention. The effects of the two winds (their directions and relative strength) have been described by two well-known models. In Bagnold's (1941) model, the limb parallel to the strongest wind is extended by the wind and sustained and enhanced by the gentler wind, which flows nearly parallel to barchans (Fig. 1a). This model was tested

in only one field experiment (Lancaster 1980) and was not successfully validated by means of numerical simulation (Parteli et al. 2007). In the second model, Tsoar (1984) proposed that the limb farthest from the gentler wind extends downwind in a manner similar to the evolution of seif dunes (Tsoar 1983), whereas the limb closest to the gentler wind is eroded (Fig. 1b).

However, it is not clear how the bi-directional winds influence the morphodynamics and morphometry of asymmetric barchans; in particular, it is not clear whether the horn nearest to or farthest from the gentler wind will extend and the direction in which it will extend. To answer this question, we developed the present study. Our goal was to determine the importance of the two winds for the evolution of asymmetric barchans by means of numerical simulations using the three-dimensional (3D) Real-Space Cellular Automaton Lattice (ReSCAL) model (<http://www.ipgp.fr/~rozier/rescal/rescal-en.html>). The results will improve our understanding of the mechanisms responsible for the formation and evolution of asymmetric barchans. Based on the results of this simulation, we can use the specific asymmetric morphologies observed elsewhere in the solar system to infer the wind regimes responsible for these forms.

The paper is organized as follows: In Sect. 2, we analyze the characteristics of the wind regime around asymmetric barchans based on the daily-scale ECMWF ERA40 (European Centre for Medium Range Weather Forecasts) reanalysis datasets from January 1958 to December 2012. In Sects. 3 and 4, we simulate the effect of wind regimes on the evolution of asymmetrical barchan dunes using a 3D ReSCAL dune model. In Sect. 5, we discuss the implications of these results.

### Characteristics of the bi-directional wind regime around asymmetric barchans

Before conducting our numerical simulation, it was necessary to understand the effects of the relative wind strengths and directions on the evolution of asymmetric barchans in nature. To do so, we used the daily-scale

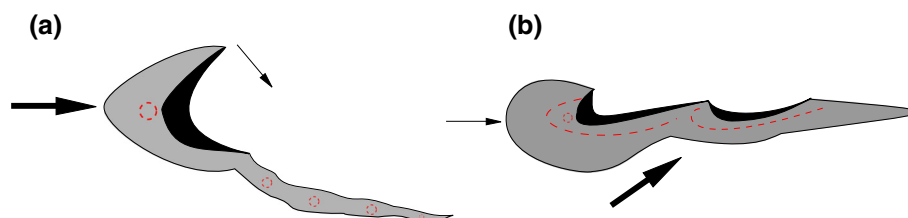


**Fig. 1** Schematic diagram of two models for the evolution of asymmetric barchans under a bi-directional wind regime. **a** Tsoar (1984). **b** Bagnold (1941). Larger arrows represent the stronger wind. Dashed lines represent higher elevations on the dune

ECMWF ERA40 reanalysis datasets (<http://apps.ecmwf.int/datasets/data/era40-daily/>) for areas of asymmetric barchans during the period from January 1958 to December 2012. Our analysis used the following technique:

For a wind speed of  $u_i$  and a wind direction  $x_i$  at time  $t_i$  and height  $z$ , with  $i = 1, 2, \dots, N$ , the wind's shear velocity ( $u_{i*}$ ) can be defined as:

$$u_{i*}^i = \frac{u_i^i k}{\log(z/z_0)} \tag{1}$$

where  $z_0 = 10^{-3}$  m represents the surface roughness length and  $k = 0.4$  is von Karman's constant. The mean shear velocity ( $u_*$ ) is:

$$u_* = \frac{\sum_{i=2}^N u_{i*}^i (t_i - t_{i-1})}{\sum_{i=2}^N \delta_i (t_i - t_{i-1})} \tag{2}$$

where

$$\delta_i = \begin{cases} 0 & \text{for } u_{i*}^i < u_c \\ 1 & \text{for } u_{i*}^i \geq u_c \end{cases} \tag{3}$$

where  $u_c$  represents the threshold shear velocity at which particles begin to be entrained, and can be determined using the formula of Iversen and Rasmussen (1999):

$$u_c = 0.1 \sqrt{\frac{\rho_s}{\rho_f} g d} \tag{4}$$

where  $g$  is the acceleration due to gravity,  $\rho_s/\rho_f$  is the ratio of grain density to fluid density, and  $d$  is the mean grain diameter.

After obtaining  $u_*$ , the saturated sand flux on a flat, erodible bed,  $Q_{\text{sat}}(u_*)$ , can be calculated using the equation of Iversen and Rasmussen (1999):

$$Q_{\text{sat}}(u_*) = 22 \frac{\rho_f}{\rho_s} \sqrt{\frac{d}{g}} (u_*^2 - u_c^2) \quad \text{for } u_* \geq u_c \tag{5}$$

Then, for a given time period around  $t_i$ , the drift potential ( $DP$ ) and the resultant drift potential ( $RDP$ ) can be calculated.

To improve our understanding of the wind's probability distribution, identify the prevailing and secondary winds, and define their relative strengths and directions, we used an expectation-maximization algorithm to fit the flux orientation distribution with a Gaussian mixture model. Thus, we replace the real flux data by a limited number of flux vectors that are characterized by an orientation  $\theta_i$  and a weight  $w_i$  with  $i = 1, 2, \dots, n_\theta$ . Thus, considering only time periods during which the wind velocity is above the critical threshold value for sediment transport (i.e.,  $u_* > u_c$ ; see Eq. 5), we assume that the probability distribution function for the wind orientation,  $P(\theta)$ , can be described by a sum of normal distributions:

$$P(\theta) = \sum_{i=1}^{n_\theta} \frac{w_i}{\sigma_i \sqrt{2\pi}} \exp\left(-\frac{(\vartheta - \theta_i)^2}{2\sigma_i^2}\right) \tag{6}$$

where  $\sigma_i$  is the standard deviation of the wind orientation at time  $i$  in direction  $\theta_i$ .

The expectation-maximization algorithm is a natural generalization of maximum-likelihood estimation for cases with incomplete data (Chuong and Batzoglu 2008). The sand flux roses in Fig. 2 show the distribution of the wind direction. The red lines in these graphs show the bimodal distribution of the wind regime in regions with asymmetric barchans. The wind orientations ( $\mu$ ) and weights ( $w$ , the ratio of the frequency of the strongest dominant wind to the gentler dominant wind) are shown for winds from the two dominant directions, along with the proportion of the total number of recorded winds from each direction (PDF). Figure 2a shows values from China's Kumtagh Desert, where the main wind comes from NW (315°), with a weight of 0.8, and the secondary wind comes from SSW (211°), with a weight of 0.2. On this basis, the ratio of the weights of the two winds is 4.0, and the angle between the two winds is 104°. Figure 2b shows values for barchans in Sudan, where the main wind comes from NE (45°), with a weight of 0.8, and the secondary wind comes from nearly the same direction (52°), with a weight of 0.2. Their weight ratio is therefore also 4.0, but the angle between these winds is only 7°. Figure 2c shows values for barchans in Qatar, where the main wind comes from NNW (343°), with a weight of 0.8, and the secondary wind is from SSE (126°), with a weight of 0.2. The weight ratio is therefore 4.0, and the angle between the winds is 217°.

The data in this figure suggest that the effect of a bi-directional wind regime on asymmetric barchans agrees with Tsor's (1984) model, as shown by the thin arrows (the gentler wind) and thick arrows (the stronger wind). The horns extend farther on the side farthest from the gentler wind, whereas the limb closest to the gentler wind is eroded. The relative degrees of erosion and extension of the two horns appear to depend on the angle between the two winds. The difference is only 7° in Sudan, so the lengths of the two horns do not differ greatly, and both horns are thick and short; however, the horn farthest from the gentler wind is slightly longer. There is a 217° difference between the winds in Qatar, so the horn farthest from the gentler wind is greatly extended, long, and thin. The horns in the barchans from the Kumtagh Desert exhibit an intermediate degree of asymmetry, with a 104° angle between the two winds.

From this analysis, the barchans formed under the influence of a dominant wind, developing two horns that extend downwind, then evolved under the influence of a

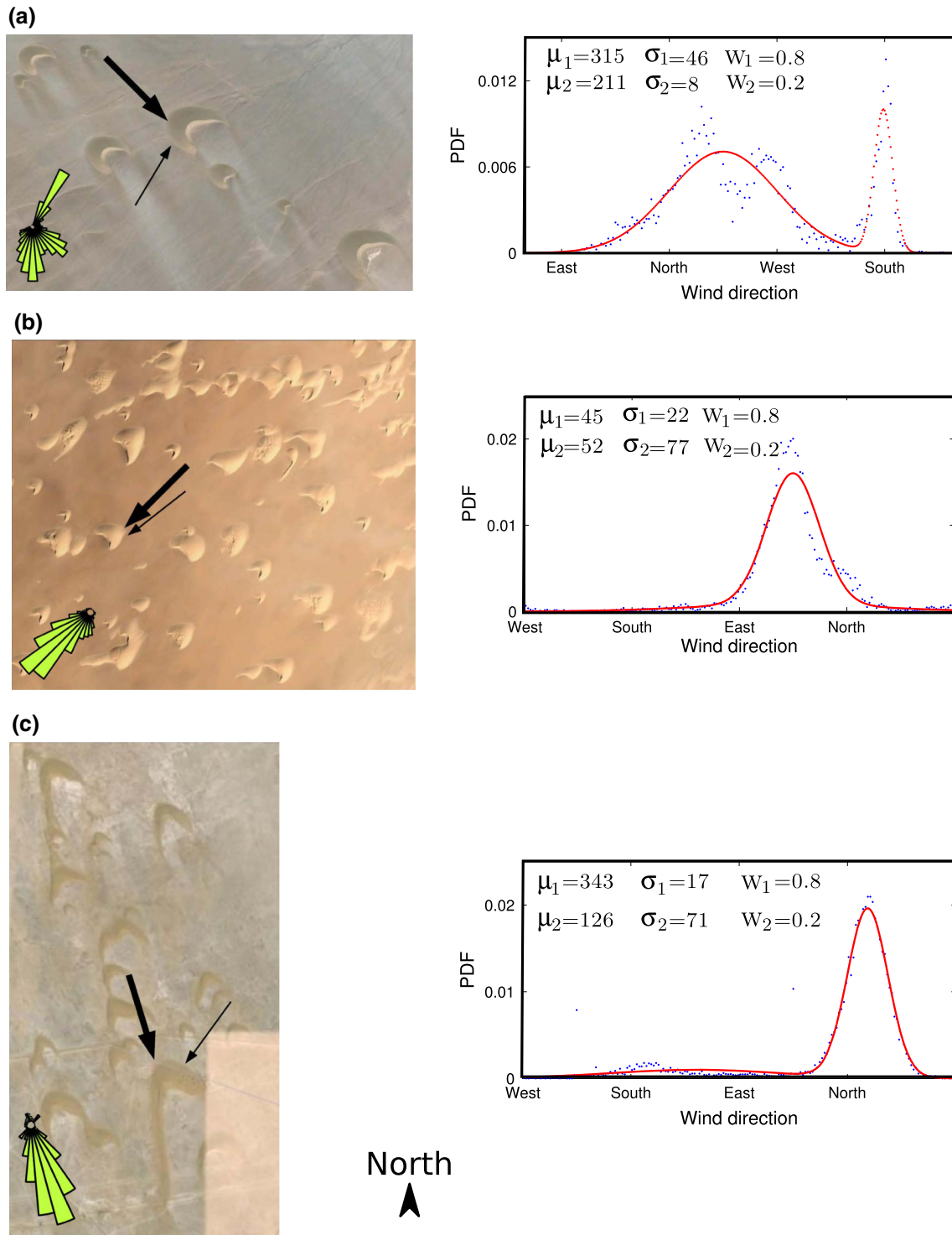


**Fig. 2** Wind regime characteristics in areas with asymmetric barchans. The wind regimes are characterized by the averaged sand flux roses (bottom left) during the period from January 1958 to December 2012 based on the daily-scale ECMWF ERA40 reanalysis datasets. The graphs on the right show the wind direction distribution. **a** China (36°39.6'N, 93°40.8'E), **b** Sudan (18°46.8'N, 25°12'E), and

**c** Qatar (25°03'N, 51°23.4'E). For dominant wind directions 1 and 2:  $\mu$  orientation (with north = 0°),  $w$  weight (ratio of the frequency of the strongest of the two dominant winds to the frequency of the gentler dominant wind),  $PDF$  proportion of the total number of winds recorded. Thin arrows represent the gentler wind; thick arrows represent the stronger wind

secondary wind, so that the horn closest to this secondary wind is eroded and the horn farthest from this gentler wind extends, leading to the evolution of asymmetric horns. The relative erosion and extension of the two horns depends on the characteristics of the wind regime. Therefore, the dynamic processes that lead to the formation of asymmetric barchans agree with Tsoar’s (1984) model.

### Cellular automaton model of dune development and initial conditions

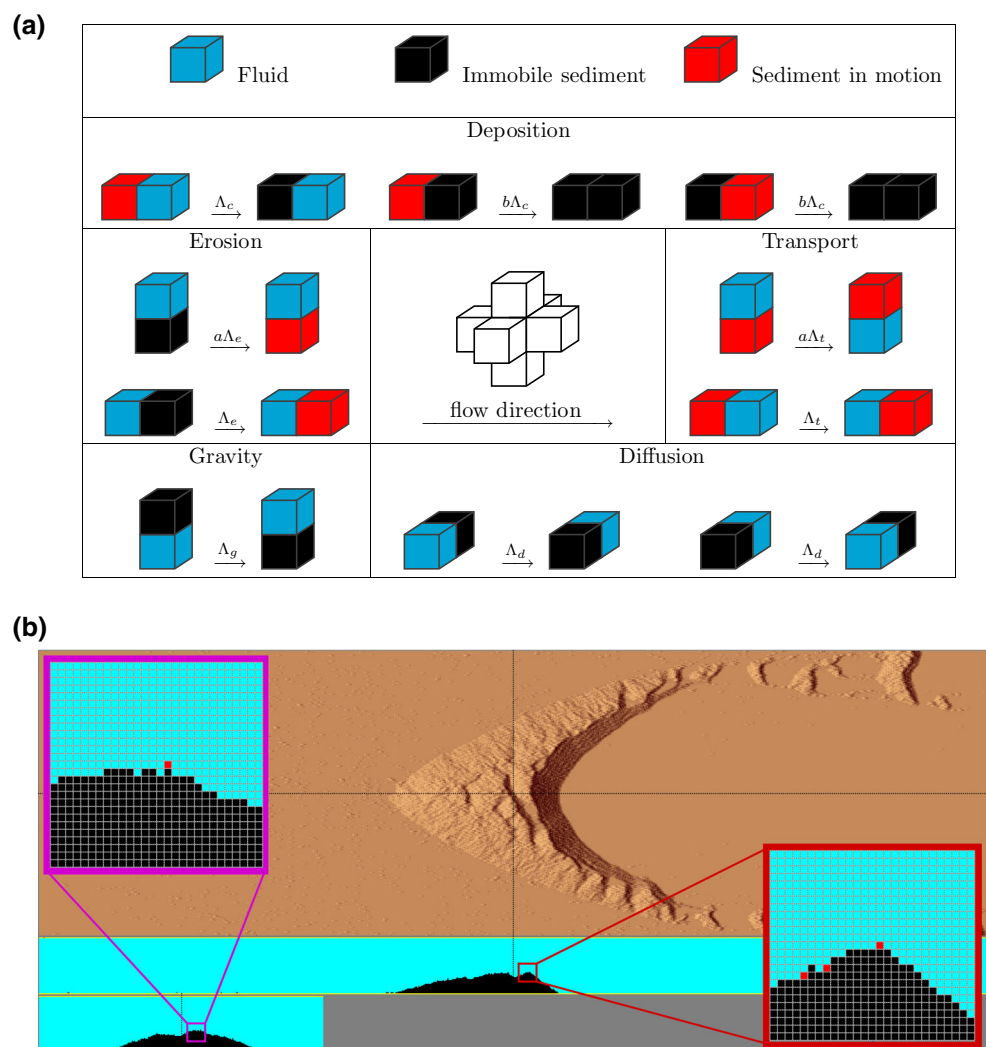
To better understand the formation and evolution mechanisms of asymmetric barchans, we used the 3D ReSCAL discrete numerical dune model (Narteau et al. 2009; Rozier and Narteau 2014). This model couples a cellular automaton model for bedform dynamics with a lattice-gas cellular automaton model for the flow dynamics. The coupling method represents the first implementation of a

permanent feedback mechanism between the flow and the bedform dynamics (Rozier and Narteau 2014).

In the model for bedform dynamics, three states (fluid, mobile sediment, and immobile sediment) and different transitions are considered to simulate erosion, transport, deposition, and the effects of gravity and diffusion (Fig. 3a); the result is a time-dependent stochastic process. The lattice-gas cellular automaton model is used to compute the flow and quantify the shear stress on the bed as a function of the topography.

Under the effect of specific wind regimes, the physical erosion, transport, and deposition processes will occur and result in a change of the bedform (i.e., the topography), and the flow will in turn change because of the topography, which will result in variations of the shear stress on the bed, which will then change the sediment transport processes. Thus, the coupling between the two models is achieved through the effect of shear stress on the dune’s topography. Using the output of the lattice-gas cellular

**Fig. 3** The 3D Real-Space Cellular Automaton Lattice (ReSCAL) dune model. **a** In the model, three states are used to reproduce the fluid, the mobile sediment, and the immobile sediment. Active transitions of doublets (the pairs of attached cubes) are used in the cellular automaton model for sediment transport. Different sets of transitions are associated with deposition, erosion, transport, and the effects of gravity and diffusion.  $\lambda$  values represent transition rates with units of frequency;  $a$  and  $b$  are positive constants. The central inset shows the direction of the flow and the orientation of the nearest neighbors in a regular cubic lattice. **b** The topography of a barchan dune in the ReSCAL dune model. *Dashed lines* represent the longitudinal and transverse vertical slices shown in the bottom half of this figure; the two insets show enlargements of individual cells



automaton, we can estimate both components of the local velocity field by averaging the velocity vectors for the fluid particles over space and time. The velocity vector  $\vec{V}$  is expressed in terms of the number of fluid particles, and we use the vector normal  $\vec{n}$  to the topography to calculate the shear stress on the bed ( $\tau_s$ ):

$$\tau_s = \tau_0 \frac{\partial \vec{V}}{\partial \vec{n}} \quad (7)$$

where  $\tau_0$  is the stress scale of the model, expressed in units of  $\text{kg } l_0^{-1} t_0^{-2}$  (where  $l_0$  represents the model's length scale and  $t_0$  represents the model's time scale). Then, we consider that the erosion rate ( $\forall_e$ ) is linearly related to the shear stress on the bed ( $\tau_s$ ) according to the following equations:

$$\forall_e = \begin{cases} 0 & \text{for } \tau_s \leq \tau_1 \\ \forall_0 \frac{\tau_s - \tau_1}{\tau_2 - \tau_1} & \text{for } \tau_1 \leq \tau_s \leq \tau_2 \\ \forall_0 & \text{for } \tau_s \geq \tau_2 \end{cases} \quad (8)$$

where  $\forall_0$  is a constant rate,  $\tau_1$  is the threshold for initiation of sediment transport, and  $\tau_2$  is a parameter to adjust the slope of the linear relationship. The excess shear stress ( $\tau_s - \tau_1$ ) is used to calculate the feedback mechanism between the shear stress on the bed and the topography.

Using this dune model, we can reproduce the large variations of natural dune patterns that appear under different wind regimes. The flow is controlled by the wind duration ( $T$ ), wind strength ( $\tau_1$ ; the higher the  $\tau_1$  value, the lower the flow velocity), and the wind direction ( $\theta$ ). Details of the ReSCAL dune model and its physical parameters are provided by Narteau et al. (2009) and Rozier and Narteau (2014).

In our simulation, the volume of the initial sand pile is held constant, with the goal of changing the wind regime (i.e., the wind strength and direction) to simulate the morphodynamics of asymmetric barchans. We used a rotating table to reproduce bi-directional wind regimes, and changed the wind strength through different wind durations ( $T$ ). In the simulation, the length, width, and height of the 3D cubic lattice were 600, 600, and 120 times  $l_0$ , respectively, where  $l_0$  is the length scale of the model. Transition rates for erosion, deposition, and transport ( $\lambda$ , with units of frequency) were held constant, and the values were the same as those used by Narteau et al. (2009). To simulate boundary conditions, we inserted a line of injection cells in the ground at the upstream border of the dune to uniformly reinject all of the sedimentary cells that have been removed at the downstream border of the dune (that is, we maintained the size of the dune rather than allowing it to shrink as cells disappeared at the downstream border), and constructed the downstream border of removal cells to eliminate all sedimentary cells that reached this limit.

## Results of the numerical simulation

During the early simulation stages, secondary patterns emerge from transient growth of some perturbations, and then propagate. The smaller patterns move faster than the larger ones, and then a coarsening and collision process occurs, with horns developing on both sides of the dune and the upstream face growing in height due to the accumulation of sedimentary cells that are systematically reinjected into the system. Finally, a single surface area is exposed to the flow, a major slip face develops on the leeward side, and the entire structure rapidly reaches a steady state in which secondary bedforms systematically develop along the horns and smaller barchan dunes regularly form and detach from the horns. The downwind extension of the two limbs clearly differs under different bi-directional wind regimes; the horn nearest to the gentler wind may be either eroded or extended, and this depends strongly on the ratio and the angle between the two winds.

Figure 4 shows the equilibrium asymmetric barchans that develop under different bi-directional wind regimes in the ReSCAL simulation. In Fig. 4a, the horns are similar under a ratio of 2 and a  $20^\circ$  angle between the two dominant winds. Figure 4b shows that the horn nearest to the gentler wind extends and the horn farthest from the gentler wind is eroded under a bi-directional wind flow with a ratio of 2 and a  $55^\circ$  angle between the two dominant winds; the two limbs are short and thick under these conditions. In contrast, the horns nearest to the gentler wind are eroded and the horn farthest from the gentler wind extends greatly when the ratio increases to 4 and the angle between the winds increases to  $80^\circ$  (Fig. 4c) and  $135^\circ$  (Fig. 4d).

According to the results of our numerical simulation, the morphometry and morphodynamics of asymmetric barchans depend strongly on the relative strengths of the two dominant winds and the angle between them. We found that there exists a critical angle. When the angle between the two winds is greater than this critical value, the effect of the bi-directional wind on the asymmetric barchans agrees with the predictions of Tsoar's (1984) model: the limb farthest from the gentler wind extends and the limb closest to the gentler wind erodes, and the length of the extension of the horns and the length difference between the two horns increase as the angle increases. When the angle is less than the critical value, the evolution of the two horns disagrees with the predictions of Tsoar's (1984) model: the horn closest to the gentler wind extends rather than the horn farthest from the gentler wind. The critical value depends on the transport ratio of the two winds. The critical values are  $70^\circ$ ,  $55^\circ$ ,  $55^\circ$ ,  $50^\circ$ , and  $50^\circ$  for transport ratios of 2, 3, 4, 5, and 6, respectively. On the other hand, when the angle between the two winds is less than  $30^\circ$  or

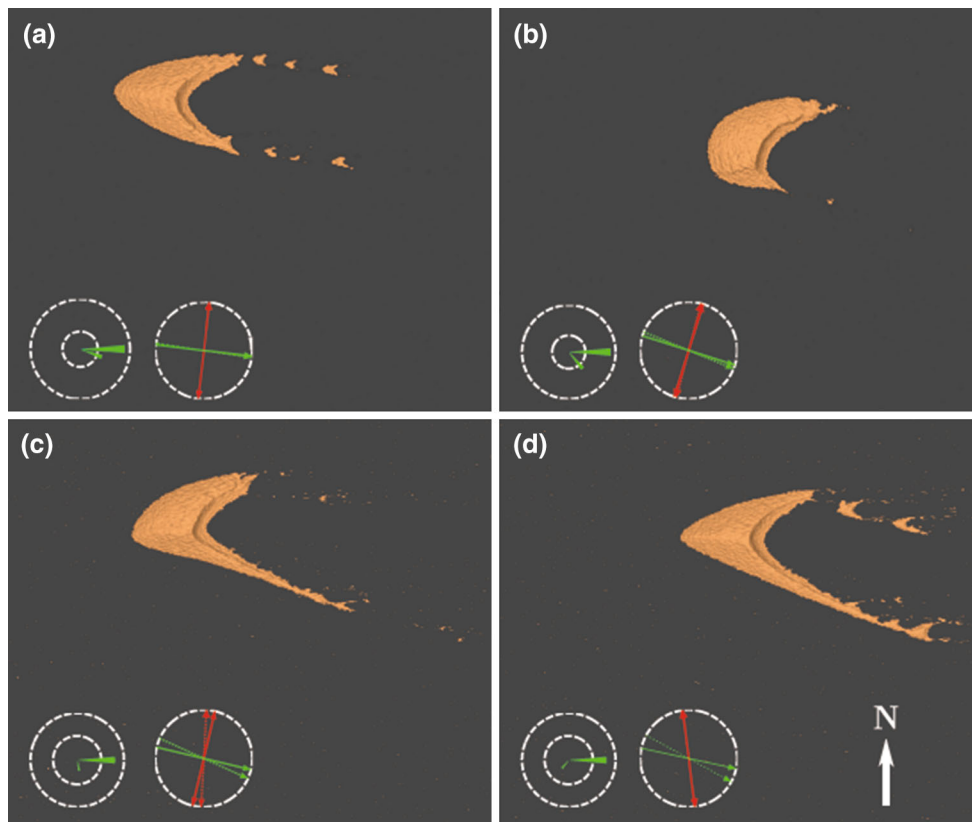


**Fig. 4** The equilibrium asymmetric barchans that developed under different bi-modal wind regimes in the ReSCAL simulation. **a**, **b** Wind strength ratios of 2 and angles between the two dominant winds of 20° and 55°, respectively. **c**, **d** Wind strength ratios of 4 and angles between the two dominant winds of 80° and 135°, respectively.

The wind roses show the wind direction regimes used in the simulation model, red lines are the orientations for which the sum of the normal components of the transport vectors reaches its maximum value (Rubin and Hunter 1987), and the *green lines* are the resultant sand flux direction based on the wind rose

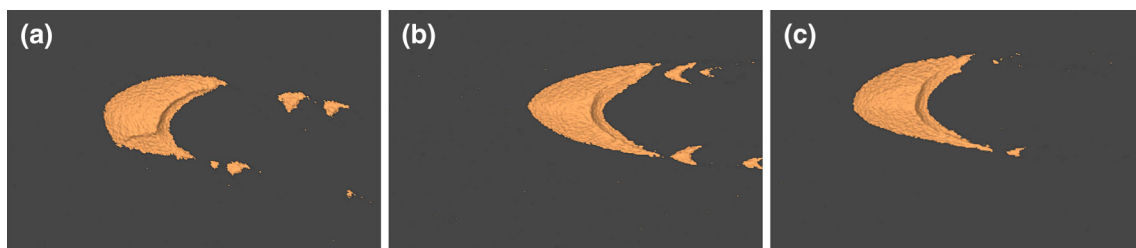


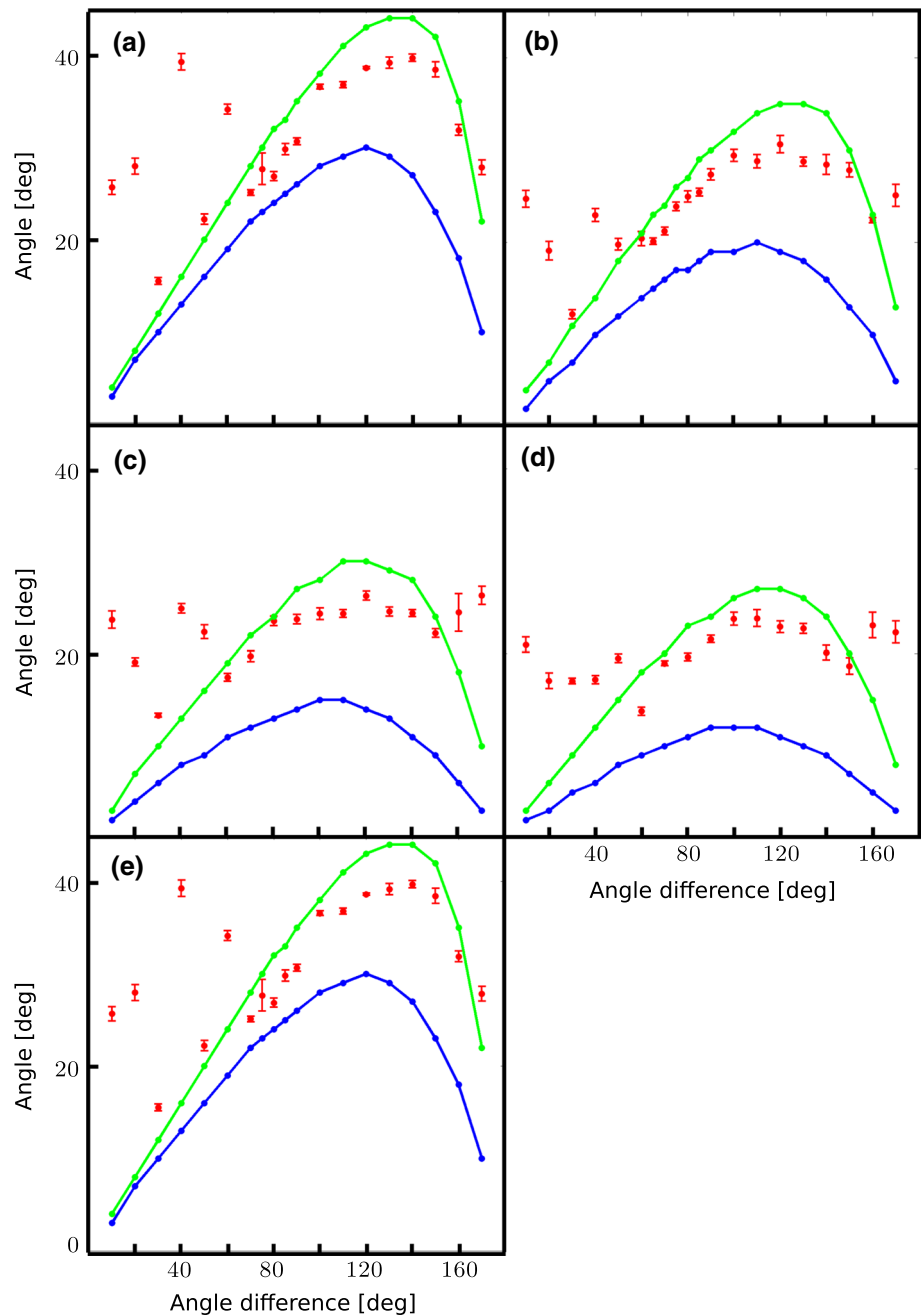
**Fig. 5** The asymmetric barchans with different angles under wind strength ratios of 5. **a** 48°, **b** 50° (critical angle), and **c** 52°, respectively

greater than 160°, the two horns are almost the same, and there is little or no asymmetry. Figure 5 is an example for transport ratio of 5 with the critical angle 50°. When the angle is 48° less than the critical value, the limb closest to the gentler wind extends and agrees with Bagnold’s model (Fig. 5a). When the angle is 52° greater than the critical value, the limb farthest from the gentler wind extends and agrees with Tsoar’s model (Fig. 5c). When the angle is 50°, the limbs are almost the same (Fig. 5b).

Additional analysis revealed that the extension direction of the horn farthest from the gentler wind results in asymmetric evolution in accordance with Tsoar’s (1984) model

under different wind regime conditions is along with the mean resultant sand flux. Figure 6 shows the extension direction of the horn farthest from the gentler wind under different bi-directional wind regimes. The green and blue lines represent the theoretical directions of the mean resultant sand flux for dune aspect ratios of  $\gamma = +\infty$  and  $\gamma = 0$ , respectively, based on specific initial wind roses (Courrech du Pont et al. 2014). The  $\gamma$  value increases with increasing angle. We also found that the extension direction of the horn farthest from the gentler wind is closer to the mean resultant sand flux considering the dune aspect ratio, this means that the dune aspect ratio has an important effect on the evolution

**Fig. 6** Extension direction of the horn farthest from the gentler wind under different wind regimes. Graphs are shown for wind strength ratios of **a** 2, **b** 3, **c** 4, **d** 5, and **e** 6. The red dots represent the direction of extension of the horn farthest from the gentler wind (mean  $\pm$  SD). The green and blue lines represent the direction of resultant sand flux for a dune aspect ratio of  $\gamma = \infty$  and  $\gamma = 0$ , respectively



direction of the horns. However, for asymmetric cases in which evolution of the horns does not follow Tsoar's (1984) model, the orientation of the horn farthest from the gentler wind is greater than the mean resultant sand flux (Fig. 6), and the two horns are almost perpendicular.

## Conclusions

In this paper, we analyzed the effect of a bi-directional wind regime on the morphodynamics of asymmetric barchans based on the models of Bagnold and Tsoar. The

morphometry and morphodynamics of asymmetric barchans depend strongly on the relative strengths and directions of the two dominant winds. There exists a critical angle between the two winds. When the actual angle is greater than this critical value, the effects of the bi-directional wind on the asymmetric barchans are in accordance with Tsoar's (1984) model: the limb farthest from the gentler wind extends and the limb closest to the gentler wind erodes, and the length difference between the two horns increases with an increasing angle. However, when the angle is less than the critical value, the evolution of the two horns does not follow Tsoar's (1984) model: the horn

closest to the gentler wind extends. The critical value depends on the transport ratio of the two winds.

By means of numerical simulation, we found that there exists a critical angle between orientations of the two winds, which decide the formation model of asymmetric barchans. The critical value is 70°, 55°, 55°, and 50° for transport ratios of 2, 3, 4, 5, and 6, respectively.

Based on our study results, the relative strengths of the two dominant winds in a bi-modal wind regime and the angle between them are responsible for the different asymmetric barchan patterns observed in nature. Thus, barchan asymmetry can be used as a proxy for the wind regime under which the dunes formed, and the dynamical mechanisms responsible for formation and evolution of the dunes (including dunes elsewhere in the solar system) can be inferred from the characteristics of their asymmetry. Another side, the barchans are the basic dunes of other kinds of dunes, which can be formed from the transformation of barchans. Therefore, we can better understand the formation mechanism of complex dunes from this study.

**Acknowledgments** We gratefully acknowledge the funding received from the National Natural Science Foundation of China (41271021 and 41130533), the UnivEarthS LabEx program (<http://www.univearths.fr/en>) of the Sorbonne Paris Cité (ANR-10-LABX-0023 and ANR-11-IDEX-0005-02), the French National Research Agency (ANR-09-RISK-004/GESTRANS and ANR-12-BS05-001-03/EXO-DUNES), and the French Chinese International laboratory SALADYN.

**Compliance with ethical standards**

**Conflict of interest** The authors declare that they have no conflict of interest.

**References**

Baas A, Nield J (2007) Modelling vegetated dune landscapes. *Geophys Res Lett*. doi:10.1029/2006GL029152

Bagnold RA (1941) *The physics of blown sand and desert dunes*. Methuen, London

Bourke MC (2010) Barchan dune asymmetry: observations from Mars and Earth. *Icarus* 205:183–197

Chuong D, Batzoglou S (2008) What is the expectation maximization algorithm? *Nat Biotechnol* 26:897–899

Courrech du Pont S, Narteau C, Gao X (2014) Two modes for dune orientation. *Geology* 42:743–746

Dong ZB, Wei ZH, Qian GQ, Zhang ZC (2010) Raked linear dunes in the Kumtagh Desert, China. *Geomorphology* 123:122–128

Finkel HJ (1959) The barchans of southern Peru. *J Geol* 67:614–647

Hersen P (2005) Flow effects on the morphology and dynamics of aeolian and subaqueous barchan dunes. *J Geophys Res*. doi:10.1029/2004JF000185

Hesp PA, Hastings K (1998) Width, height and slope relationships and aerodynamic maintenance of barchans. *Geomorphology* 22:193–204

Iversen J, Rasmussen K (1999) The effect of wind speed and bed slope on sand transport. *Sedimentology* 46:723–731

King W (1918) Study of a dune belt. *Geography J* 51:16–33

Kocurek G, Ewing R (2005) Aeolian dune field self-organization—implications for the formation of simple versus complex dune-field patterns. *Geomorphology* 72:94–100

Lancaster N (1980) The formation of seif dunes from barchans—supporting evidence for Bagnold’s model from the Namib desert. *Geomorphology* 24:160–167

Lancaster N (1995) *Geomorphology of desert dunes*. Routledge, New York

Lv P, Dong ZB (2013) The pressure-field characteristics around porous wind fences: results of a wind tunnel study. *Environ Earth Sci* 68:947–953

Lv P, Dong ZB (2014) The status of research on the development and characteristics of mass-flux-density profiles above wind-eroded sediments: a literature review. *Environ Earth Sci* 71:5183–5194

Lv P, Narteau C, Dong ZB, Zhang ZC, Courrech du Pont S (2014a) Emergence of oblique dunes in a landscape-scale experiment. *Nat Geosci* 7:99–103

Lv P, Dong ZB, Mu QS, Luo WY (2014b) An analysis of drag force on wind of shrubs simulated in a wind tunnel. *Environ Earth Sci* 71:125–131

McKee E (1966) Structures of dunes at White Sands National Monument. New Mexico and a comparison with structures of dunes from other selected areas. *Sedimentology* 7:1–60

McKee E (1979) Introduction to a study of global sand seas. In: *A Study of Global Sand Seas*. E. McKee (eds), pp 3–19

Narteau C, Zhang D, Rozier O, Claudin P (2009) Setting the length and time scales of a cellular automaton dune model from the analysis of superimposed bed forms. *J Geophys Res* 114:F03006. doi:10.1029/2008JF001127

Parteli E, Duran O, Herrmann H (2007) Reply to comment on ‘minimal size of a barchan dune’. *Phys Rev E*. doi:10.1103/PhysRevE.76.063302

Pye K, Tsoar H (1990) *Aeolian sand and sand dunes*. Unwin Hyman, London

Radebaugh J, Lorenz R, Farr T, Paillou P, Savage C, Spencer C (2010) Linear dunes on titan and earth: initial remote sensing comparisons. *Geomorphology* 121:122–132

Rim M (1958) Simulations by dynamical model, of sand tract morphology occurring in Israel, 7-G. *Bull. Res. Council, Israel*

Rozier O, Narteau C (2014) A real space cellular automaton laboratory. *Earth Surf Proc Land* 39:98–109

Rubin D, Hunter R (1987) Bedform alignment in directionally varying flows. *Science* 237:276–278

Tsoar H (1983) Dynamic processes acting on a longitudinal (seif) sand dune. *Sedimentology* 30:567–578

Tsoar H (1984) The formation of seif dunes from barchans—a discussion. *Zeit. für Geomorphology* 28:99–103